Parallel-pumping studies of magnon damping in MnF_2

J. Barak
Solid State Physics Department, Israel Atomic Energy Commission, Soreq Nuclear Research Center, Yavne 70600, Israel

S. M. Rezende
Departamento de Fisica, Universidade Federal de Pernambuco, Recife, Brasil and Department of Physics, University of California, Santa Barbara, California 93106

A. R. King and V. Jaccarino
Department of Physics, University of California, Santa Barbara, California 93106
(Received 5 November 1979)

The relaxation rate of electronic magnons with wave vectors $\vec{k}$ smaller than 0.03 k_{ZB} has been measured as a function of temperature and $\vec{k}$, using the technique of parallel pumping. The experiments utilized high magnetic fields to probe the region just below the antiferromagnetic spin-flop transition, which then involves magnons with microwave frequencies. The measured relaxation rates in the temperature range 1.4 to 10 K span the range 10^5–10^6 sec^{-1}, and show two distinct temperature dependences. At lower temperatures a nearly linear T dependence, and at higher ones a T^4 dependence, are observed. Magnon-relaxation calculations reveal that at lower temperatures the three-magnon dipole-dipole interaction is probably responsible for the damping, whereas four-magnon exchange and anisotropy interactions prevail at the higher ones, in satisfactory agreement with experiment. The latter result is in agreement with antiferromagnetic resonance measurements in MnF_2, which showed the linewidth to be accurately described by the four-magnon process for $T > 5$ K.

I. INTRODUCTION

One of the most interesting characteristics of the dynamics of magnetic systems is the manner by which energy is transferred from their elementary excitations to the lattice. This is characterized by the magnon damping, or relaxation rate, which can be measured by various experimental methods. For example, in the inelastic scattering of slow neutrons, the spin-wave relaxation rate is measured directly from the energy width of the scattering cross section. Because of the limited resolution of the neutron data, this technique has been restricted to magnons with $\vec{k}$ near the edge of the Brillouin zone (k_{ZB}) and to temperatures not much smaller than the ordering temperature (T_c), for the damping would otherwise not be large enough to measure with any precision. Only recently high-resolution neutron scattering has been used to yield magnon-damping measurements over somewhat more extensive wave vector $\vec{k}$ and temperature ranges,[1] encompassing now the regions $\vec{k} > 0.1 k_{ZB}$ and $T > 0.2 T_c$. Other techniques used to measure large-wave-vector magnon damping include magnon sideband optical absorption[2] and two-magnon light scattering.[3,4] Since the information on the magnon damping in these experiments is extracted from the width of the interacting two-magnon line shape, it provides information primarily on the zone-edge magnons, and its accuracy is limited.

The damping of long-wavelength magnons can best be measured by means of several parametric excitation processes, amongst which the most widely employed are the perpendicular-pumping Suhl instabilities,[5] the phonon-pumping,[6] and the parallel-pumping techniques.[7,8] The parallel-pumping process, so called because the rf magnetic field is applied parallel to the static field, allows selective excitation of a chosen magnon pair and is the most widely used technique to study small-$\vec{k}$ magnons. The relaxation rate is proportional to the threshold rf field above which there is a sudden buildup of the spin waves as determined by energy and momentum conservation conditions. The technique is generally restricted to small-$\vec{k}$ magnons and temperatures much smaller than the ordering temperature because of the limitations in available microwave power at higher frequencies.

Although parallel-pumping experiments were performed on ferromagnetic magnons many years ago, allowing a detailed theoretical interpretation of the data in terms of magnon-relaxation theory,[9,10] the same is not true for antiferromagnetic systems. Several of the low-anisotropy antiferromagnets, such as $RbMnF_3$, $CsMnF_3$, and $KMnF_3$, whose small-$\vec{k}$ magnon frequencies fall in convenient microwave ranges, have anisotropy fields H_A much smaller than the exchange field H_E, which necessitates using

prohibitively large threshold rf fields for pumping two electronic magnons. Instead, information on the electronic-magnon damping in these materials has been obtained by parametrically pumping an electronic-nuclear magnon pair.[11,12] However, the interpretation of these experiments is difficult because one must first know the nuclear-magnon-damping mechanisms as obtained by yet other pumping processes and convolute this information to obtain the electronic-magnon damping. Additional complications in these materials arise from the fact that small strain-induced inhomogeneities produce large fluctuations in the anisotropy field, resulting in non-momentum-conserving magnon-scattering processes.[13,14] Very detailed parallel-pumping studies have been made in $CuCl_2 \cdot 2H_2O$,[15] but in this case the crystal and magnetic structure are sufficiently complex as to preclude detailed analysis.

In this paper we present the study by parallel pumping of the damping of long-wavelength magnons in the nearly ideal antiferromagnet MnF_2. In many respects MnF_2 is the ideal choice of material for these experiments, since the magnetic structure and excitation are simple and well known. Furthermore, detailed measurements of the antiferromagnetic resonance (AFMR) linewidth versus temperature have been made,[16] and are very well explained by various magnon-relaxation processes.[17] Therefore, we expect that the extension of the latter calculations to $k \neq 0$ should accurately describe the theoretical situation and allow a detailed quantitative comparison between experiment and theory.

The relaxation data were taken by the parallel-pumping method as a function of temperature, frequency, and magnetic field. Due to both the relatively high ellipicity of the spin precession and the non-negligible value of $H_A/H_E \simeq 0.15$ in this material, it was possible to pump two *electronic* magnons directly, in contrast to the previous studies on the $KMnF_3$, $RbMnF_3$, and $CsMnF_3$ systems discussed above.

Since all the parameters of MnF_2 are accurately known, we have been able to interpret the data using magnon-relaxation theory. This constitutes the first example of a detailed analysis of a parallel-pumping experiment in an antiferromagnet. We have found that at low temperatures the three-magnon dipolar interaction can relax a small-$\vec{k}$ antiferromagnetic magnon and that this process is essential to explain the data, in addition to the usual four-magnon exchange and anisotropy interactions.

Section II describes the details of the experiments. The main experimental results are presented in Sec. III. Section IV is devoted to the magnon-relaxation calculations resulting from three- and four-magnon interactions. In the last section the theoretical interpretation of the data is discussed, and the effects of sample size are described. In the Appendix we present a quantum-mechanical derivation of the threshold field for parallel pumping of electronic magnons in antiferromagnets.

II. EXPERIMENTS

Experiments were done at microwave frequencies in the range 12–18 GHz on the down-going frequency branch of samples with the c axis accurately aligned along the field of a superconducting solenoid. Two electronic magnons, each with half the microwave frequency, were parametrically pumped, and the relaxation data inferred from measurements of the threshold power. This was determined by applying pulsed microwave power of a few watts for about 10 μsec, and measuring the power level above which nonlinear behavior was observed. The latter was evidenced by a nonlinear buildup of the absorption, with a time constant decreasing with increased power, followed by an oscillatory behavior at high power levels, similar to that observed in ferromagnets.[18] Sample-heating effects were avoided by decreasing the pulse repetition rates until no effect on the signal due to the pulse repetition rate could be observed. The measurements were made at temperatures between 1.4 and 10 K, in fields just below the spin-flop field $H_c = 92.94$ kOe at 4.2 K, in MnF_2.

The microwave oscillator was a yttrium iron garnet (YIG)-tuned sweep generator operated cw at a fixed frequency, delivering about 10 mW over the frequency band 12–18 GHz. Its output was switched with a coaxial *PIN* diode with a rise time of 20 nsec and on/off ratio of 80 dB, and attenutated with a broadband coaxial step attenuator. The requisite high rf power was obtained by amplifying this signal with a *Ku*-band traveling-wave-tube (TWT) amplifier, which delivered 10 W of saturated power between 12 and 18 GHz. The TWT-amplifier gain was sufficient to deliver full power output over the whole operating band, except close to 18 GHz. Following the amplifier output, a *Ku*-band wave-guide system was used, with isolator, calibrated attenuator, and dual-directional couplers, attenuators, and detectors for measuring incident and reflected powers. A stainless-steel wave-guide section was used in the Dewar, and the sample was mounted in a silver-plated cylindrical TE_{011} cavity with variable iris coupling. Because of space limitations in the superconducting solenoid, the empty cavity was designed to resonate somewhat above 18 GHz, and was then filled with various dielectrics to lower the frequency: Powdered wax for 18 GHz, wax of $\epsilon = 2.35$ for 15 GHz, and sulfur of $\epsilon = 3.5$ for 12 GHz were used for that purpose. The strength of the threshold rf magnetic field h_c in the cavity was determined from the known incident power, the measured waveguide attenuation and cavity Q. It was then related to the magnon-relaxation rates in a manner to be discussed.

Three different samples of MnF_2 were used, all of which were grown by N. Nighman at the Univ. Calif. at Santa Barbara. Sample 1 consisted of pure MnF_2, shaped in the form of a rod with diameter 1.5 mm and length 4 mm, with the crystalline c axis parallel to the rod axis. Sample 2 (also pure MnF_2) was shaped as a sphere of radius 0.6 mm, and polished to a mean surface roughness of about 1 μm. Sample 3 was an unshaped crystal of $Mn_{0.98}Co_{0.02}F_2$ of approximately 1 mm^3 in volume.

The samples were mounted on the end of a sapphire rod, coaxial with, and thermally anchored to, one end of the microwave cavity. The temperature was measured with a capacitance thermometer, mounted in a hole in the cavity wall, and controlled with a standard capacitance bridge and temperature controller. A variable heat leak to the surrounding liquid-helium bath was maintained by varying the pressure of helium exchange gas inside the single-wall central tube of the Dewar.

Samples were aligned *in situ* by observing AFMR, and tilting the sample along with the entire cavity, in order to decrease the resonant field to as low a value as possible. To accomplish this, a set of tilting screws was built into the sample holder, with control rods extending out the top, and a short section of flexible waveguide was included just above the cavity.

Magnetic fields were provided by a 0–140-kOe GE superconducting solenoid, and measured by a broad-band NMR magnetometer probe, mounted in the cavity wall, to an accuracy of about 1 Oe.

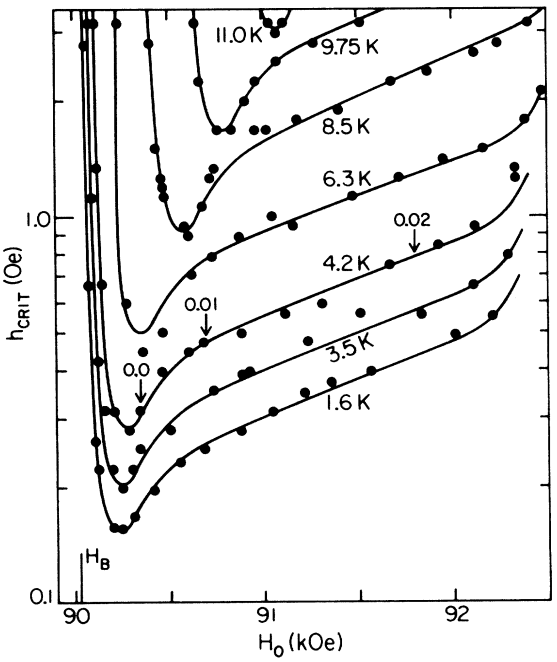

FIG. 1. Threshold rf field as a function of dc field for parallel pumping of two electronic magnons with frequency 7.59 GHz in MnF_2 at various temperatures. The sample is rod-shaped (No. 1) and $H_0 \| c$ axis and is just below the spin-flop transition. The value H_B corresponds to the $k=0$, $\theta=0$ mode at 4.2 K. The numbers indicate the values of the normalized wave vectors k/k_{max} which are "tuned in" by the magnetic field at the frequency 7.59 GHz.

III. RESULTS

Threshold-field results, similar to the "butterfly" curves obtained in earlier parallel-pumping experiments in ferromagnets,[9] were measured in MnF_2 just below the spin-flop field. Figure 1 shows the data for a pumping frequency of 15.18 GHz at various temperatures for the rod-shaped sample No. 1. Similar curves were obtained for all samples and at all frequencies used. The behavior of the magnon damping can be inferred qualitatively from the expression for the threshold field $h_{c\vec{k}}$ derived in the Appendix. For H_A, $\omega_{\alpha k}/\gamma \ll H_E, H_c$ Eq. (A9) gives

$$h_{c\vec{k}} = \frac{\omega_{\alpha k}(1/\gamma T_{\vec{k}})}{\gamma \pi M \sin^2\theta_{\vec{k}}} \left(\frac{2H_E}{H_A}\right)^{1/2} , \tag{1}$$

where $\omega_{\alpha k}$ is the "down-going" magnon frequency, $1/T_{\vec{k}}$ is its relaxation rate, $\theta_{\vec{k}}$ is the angle between the wave vector and the dc field, γ is the gyromagnetic ratio, and M is the sublattice magnetization. The dispersion relation for small-$\vec{k}$ magnons, with account taken for the Zeeman, exchange, anisotropy, Lorentz, and dipolar interactions,[19] is, in the limit

$$H_0(H_c - H_0) \gg 2\pi M H_A \text{ and } H_A \gg H_E(1-\gamma_k^2),$$

$$\omega_{\alpha k}/\gamma = [H_c^2 + 4\pi M H_A(\sin^2\theta_k - \tfrac{2}{3}) + H_E^2(1-\gamma_k^2)]^{1/2} - H_0 , \tag{2}$$

where, for MnF_2

$$\gamma_k = \cos(\tfrac{1}{2}k_x a)\cos(\tfrac{1}{2}k_y a)\cos(\tfrac{1}{2}k_z c) .$$

The AFMR frequency is obtained from Eq. (2) by setting $k=0$ and replacing the $\sin^2\theta_k$ term by one containing the appropriate transverse demagnetizing factor. For a spherical sample this latter term just cancels the Lorentz contribution, and the AFMR frequency at $H_0=0$ becomes $\omega_0/\gamma = H_c = (2H_E H_A + H_A^2)^{1/2}$. At low temperatures the temperature dependence of the magnon frequencies is almost entirely contained in H_c. In MnF_2, near the spin-flop field, H_c can be very well described at $T < 20$ K by[20]

$$H_c(T) = 92.88 + (9.5\times10^{-4})T^{2.85} , \tag{3}$$

with $H_c(T)$ in kOe.

The long-wavelength spin-wave manifold is shown in Fig. 2 for MnF_2 at 4.2 K with the following param-

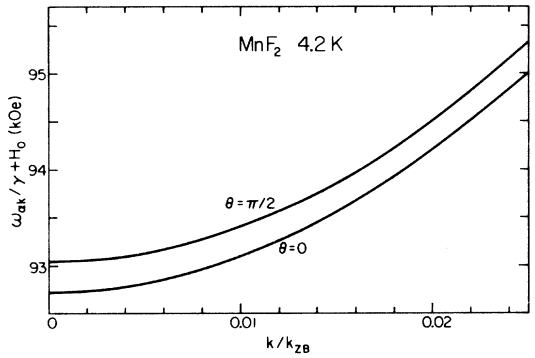

FIG. 2. Long-wavelength magnon dispersion relation in MnF_2 at 4.2 K. θ is the angle between the wave vector and the applied field $H_0 \| c$ axis. The wave vectors are normalized with respect to values at the Brillouin-zone boundary in the specific direction in k-space.

eters[21] used: $H_E = 526$ kOe, $H_A = 8.02$ kOe, and $M = 592$ Oe. Note that, since the magnon frequency decreases with increasing field, the butterfly curves of Fig. 1 are reversed in field with respect to the usual ones for ferromagnets.[9] At higher fields, but still below H_c, $\theta_k = \frac{1}{2}\pi$ magnons are accessible for pumping, as illustrated in Fig. 1. Since they have the highest precession ellipticity and consequently the lowest threshold, they go unstable first and tend to dominate the parametric excitation process. The high-field side of the curves in Fig. 1 thus tend to reflect the relaxation rate of $\frac{1}{2}\pi$ magnons. The behavior of the high-field side indicates that the relaxation rate increases with increasing wave vector and temperature as one would expect. As the field is lowered and approaches the bottom of the band, k tends to zero for $\frac{1}{2}\pi$ magnons. Consequently, below this point only $k \simeq 0$, $\theta_k < \frac{1}{2}\pi$ magnons are accessible for pumping. Since they have smaller ellipticity than the $\frac{1}{2}\pi$ magnons their threshold is correspondingly higher and the curves rise sharply. At fields below $H_B = 90.02$ kOe at 4.2 K, no magnons can be excited, and the threshold tends to infinity.

An interesting feature of the curves in Fig. 1 is the pronounced dip displayed at the bottom. This dip is sample dependent, as clearly demonstrated in Fig. 3. The rod-shaped sample No. 1 has a pronounced dip at all temperatures. The smaller sphere, sample No. 2, has a dip only at higher temperatures. The origin of this feature will be discussed later.

The highest field at which data can be obtained is limited by the onset of the mixed-phase region in which antiferromagnetic (AF) and spin-flop (SF)

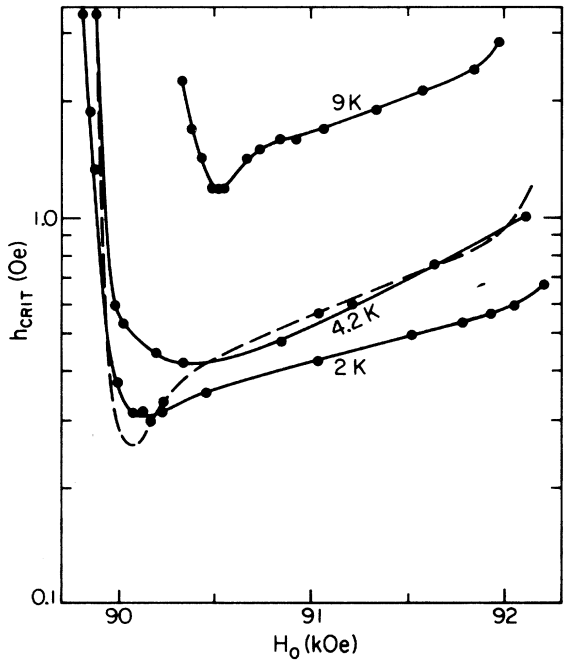

FIG. 3. Comparison between the threshold field vs applied dc field for the rod-shaped sample No. 1 at $T = 4.2$ K (dashed line), and the sphere No. 2 (solid line) at various temperatures.

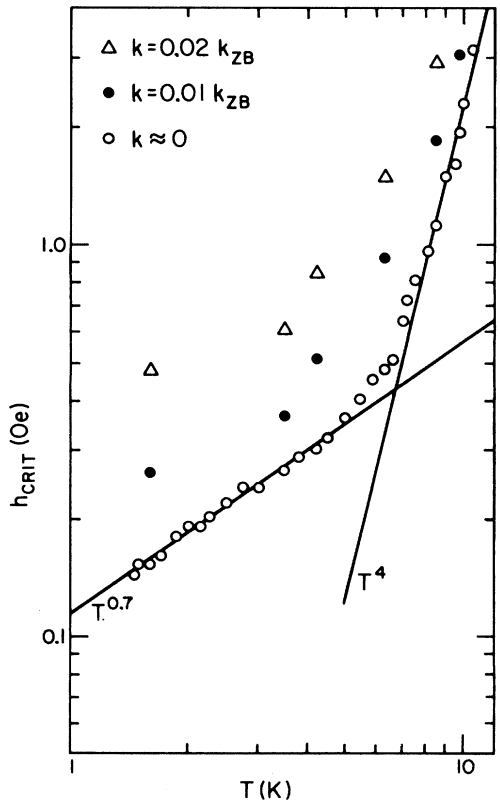

FIG. 4. Temperature dependence of the magnon-relaxation rates for various wave vectors at fixed frequency in MnF_2. The data are extracted directly from Fig. 1 and Eqs. (1)–(3), with additional data points at $k \sim 0$ taken at the bottom of the dip.

domains coexist.[22] The displacement of the butterfly curves toward higher fields at higher temperatures reflects the temperature dependence of the spin-flop phase transition,[20] and with it, the low-lying magnon frequencies. Using the known temperature dependence for the frequency, from Eq. (3), one can extract the relaxation data for various k values at different temperatures, as indicated in Fig. 1. Assuming that the threshold measured corresponds to the $\theta = \frac{1}{2}\pi$ mode, a question to which we shall return later, we obtain the data shown in Fig. 4. Two distinct temperature dependences are observed. For $T < 5$ K the damping rate follows a temperature dependence close to $T^{0.7}$. For higher temperatures it becomes a T^4 dependence, a result which has been previously observed for the $k = 0$ uniform mode.[16]

IV. THEORY OF ANTIFERROMAGNETIC MAGNON RELAXATION

Previous treatments[23,24] of magnon damping in antiferromagnets in the AF phase have neglected the three-magnon dipole-dipole interaction. This process is usually unimportant because of the difficulty in conserving both energy and momentum as a result of the gap in the magnon dispersion relation. Since this process has been shown[10] to dominate the relaxation of small-k ferromagnetic magnons at low temperatures, it might be expected to play an important role in the damping of antiferromagnetic magnons at fields near the AF $\rightarrow$SF transition, where the gap is small, as is the case of the present experiments. This is supported by the data of Fig. 4, which show the abrupt change in slope of the damping rate as a function of temperature. The T^4 dependence observed in the relaxation of the $k = 0$ uniform mode was shown[17] to arise from four-magnon scattering processes involving both the exchange and anisotropy interactions. For $k \neq 0$, but still small compared to the Brillouin-zone edge, one would expect the four-magnon scattering to exhibit the same T^4 dependence.

At lower temperatures the relaxation rate would tend to be dominated by allowed scattering processes involving fewer than four magnons, because these would give a weaker T dependence. For the $k = 0$ mode no three-magnon process can conserve both energy and momentum, but for $k > 0$, it is allowed for certain values of k and of the gap. In ferromagnets the dipolar three-magnon scattering has a linear T dependence,[10] and one might expect a similar behavior in the antiferromagnet.

To calculate the damping of magnons so as to make comparison with experimental results, we consider a Hamiltonian with Zeeman, magnetic dipole-dipole and isotropic exchange interactions. When the spin operators are expanded in terms of the Holstein-Primakoff a_k's and b_k's one obtains

$$\mathcal{H} = E_0 + \mathcal{H}^{(2)} + \mathcal{H}^{(3)} + \mathcal{H}^{(4)} + \cdots \quad . \tag{4}$$

The presence of the dipolar interaction in $\mathcal{H}$ complicates the form of the quadratic part $\mathcal{H}^{(2)}$, introducing terms like $a_k a_{-k}$ and $a_k b_{-k}^{\dagger}$ in addition to the ones which would result from a single-ion form for the anisotropy. To obtain a detailed expression for the magnon frequency including the effect of the dipole interaction, as given by Eq. (2), a 4×4 transformation matrix is required for the diagonalization of $\mathcal{H}$, as is shown in the Appendix. However, since the additional terms in the transformation are small compared to the ones required to diagonalize the Hamiltonian with Zeeman, exchange, and single-ion anisotropy interactions, we neglect them in the higher-order terms in $\mathcal{H}$. This has a small effect in the vertices of the magnon interactions because they are made up of products of the transformation coefficients and there are no cancellations of large terms.

One further simplification is made in the following calculations. Since our experiments involved low-frequency α_k magnons at low temperatures, we neglect all interaction processes containing the "up-going"-frequency β_k magnons.

The scattering terms of the Hamiltonian in Eq. (4) will then have the form

$$\mathcal{H}^{(3)} = \sum_{k_1,k_2,k_3} (C_{1,2,3}\alpha_{k_1}\alpha_{k_2}\alpha_{k_3}^{\dagger} + \text{H.c.})\Delta(\vec{k}_1 + \vec{k}_2 - \vec{k}_3) \quad , \tag{5}$$

$$\mathcal{H}^{(4)} = \sum_{k_1,k_2,k_3,k_4} C_{1,2,3,4}\alpha_{k_1}\alpha_{k_2}\alpha_{k_3}^{\dagger}\alpha_{k_4}^{\dagger} \times \Delta(\vec{k}_1 + \vec{k}_2 - \vec{k}_3 - \vec{k}_4) \quad . \tag{6}$$

The relaxation rate for mode k_1 will be calculated from the general result[17] for a process in which N magnons are destroyed and M are created.

$$\eta_1^{(N+M)} = \frac{2\pi}{\hbar^2}\frac{1}{\bar{n}_1}\sum_{k_1,k_2,\ldots} |C^{(N+M)}|^2(\bar{n}_2+1)\cdots \times(\bar{n}_N+1)\bar{n}_{N+1}\cdots \times \bar{n}_{N+M}\delta(\omega)\Delta(\vec{k}) \quad . \tag{7}$$

A. Three-magnon dipolar confluence relaxation

The only three-magnon relaxation process for small-$\vec{k}$ magnons in which energy and momentum can be conserved is the confluence process. The dipolar confluence process for magnon relaxation in antiferromagnets has previously been considered in connection with nuclear relaxation.[25] We write the

three-magnon part of the dipolar Hamiltonian[25]

$$\mathcal{H}_d^3 = -2\pi g\mu_B M(2/NS)^{1/2} \sum_{k_1,k_2,k_3} [(k_1^- k_1^z/k_1^2)(a_1 + b_1^\dagger)(a_2^\dagger a_3 - b_2 b_3^\dagger) + \text{H.c.}]\Delta(\vec{k}_1 - \vec{k}_2 + \vec{k}_3) \quad , \tag{8}$$

where a_1 and b_1 are shorthand notations for a_{k_1} and b_{k_1}, N is the number of spins in each sublattice, and $g\mu_B = \hbar\gamma$. Making the usual Holstein-Primakoff transformation to normal-mode variables

$$a_k = u_k\alpha_k - v_k\beta_k^\dagger, \quad b_k = u_k\beta_k - v_k\alpha_k^\dagger$$

and dropping all terms involving upper branch magnons β_k and $\beta_k^\dagger$, we have

$$\mathcal{H}_d^{3'} = -2\pi g\mu_B M(2/NS)^{1/2} \sum_{k_1,k_2,k_3} [(k_1^- k_1^z/k_1^2)(u_1 - v_1)(v_2v_3 - u_2u_3)\alpha_1^\dagger\alpha_2^\dagger\alpha_3^\dagger + \text{H.c.}]\Delta(\vec{k}_1 - \vec{k}_2 + \vec{k}_3) \quad . \tag{9}$$

The neglect of all but the α magnons is justified since only they are accessible at microwave frequencies, and then only in high magnetic fields. In the rather low temperatures in which the experiments were done, the population of β modes is negligible compared to the α modes. Substituting this Hamiltonian into Eq. (7), we find for the three-magnon relaxation rate

$$\frac{1}{T_k} = \frac{\pi}{2\hbar^2} \sum_{k_1,k_2,k_3} |C|^2(1 + \bar{n}_2)\bar{n}_3/\bar{n}_1\Delta(\vec{k}_1 + \vec{k}_2 - \vec{k}_3)\delta(\omega_1 + \omega_2 - \omega_3) \quad , \tag{10}$$

where

$$C = 4\pi g\mu_B M(NS)^{-1/2}[(k_2^- k_2^z/k_2^2)(u_2 - v_2)(u_1u_3 - v_1v_3) + (k_1^- k_1^z/k_1^2)(u_1 - v_1)(u_2u_3 - v_2v_3)] \quad .$$

In order to eliminate analytically as many variables as possible for general directions of $\vec{k}_1$, we transform to a primed set of coordinates with $z' \| \vec{k}_1$. Assuming $\vec{k}_1$ makes an angle θ_1 with respect to z in the xz plane, and k_2 makes an angle θ' with respect to z' in the $x'z'$ plane, we make a transformation through the following Euler angles: θ_1, 0, ψ. We then have the $|C|^2$ in terms of the new variables

$$\begin{aligned} |C|^2 = {} & \sin^2\theta_1\cos^2\theta_1 C_1^2 + 2C_1C_2[\sin^2\theta_1\cos\theta_1\sin^2\theta'\sin\psi\cos\psi + \sin\theta_1\cos^2\theta_1\sin\theta'\cos\theta'\cos\psi] \\ & + C_2^2[\sin^2\theta'\cos^2\psi + \sin^2\theta'\cos^2\theta_1\sin^2\psi - 2\sin\theta_1\cos\theta_1\sin\theta'\cos\theta'\sin\psi + \sin^2\theta_1\cos^2\theta'] \\ & \times [\sin^2\theta_1\sin^2\theta'\sin^2\psi + 2\sin\theta_1\cos\theta_1\sin\theta'\cos\theta'\sin\psi + \cos^2\theta_1\cos^2\theta'] \quad , \end{aligned} \tag{11}$$

where

$$C_1 = (u_1 - v_1)(u_2u_3 - v_2v_3), \quad C_2 = (u_2 - v_2)(u_1u_3 - v_1v_3) \quad .$$

Before proceeding further, we notice that ω_k for small $\vec{k}$ in MnF_2 is very nearly isotropic, except for the small term due to the anisotropy in the dipolar interaction. We retain this term in the magnon $\vec{k}_1$ under study, since in the region very near spin-flop in which the experiments are done, it is a significant part of its energy. However, we expect that the important scattered magnons $\vec{k}_2$ and $\vec{k}_3$ to have energies much larger than that of $\vec{k}_1$, making the dipolar term relatively unimportant. Moreover, since the important $\vec{k}_2$ and $\vec{k}_3$ should be much larger than $\vec{k}_1$, $\vec{k}_2$ and $\vec{k}_3$ will be nearly parallel. Thus, whatever are the dipolar contributions to ω_2 and ω_3, they will be nearly equal, and cannot significantly alter the energy conservation.

With this assumption, we can now integrate over the angle ψ, obtaining the result

$$\begin{aligned} \frac{1}{2\pi}\int d\psi|C|^2 = {} & C_1^2\sin^2\theta_1\cos^2\theta_1 \\ & + C_2^2(\tfrac{1}{8}\sin^4\theta'\sin^2\theta_1 + \tfrac{3}{8}\sin^4\theta'\sin^2\theta_1\cos\theta_1 + \tfrac{1}{2}\sin^2\theta'\cos^2\theta'\cos^4\theta_1 - 2\sin^2\theta'\cos^2\theta'\sin^2\theta_1\cos^2\theta_1 \\ & + \tfrac{1}{2}\sin^2\theta'\cos^2\theta'\sin^4\theta_1 + \tfrac{1}{2}\sin^2\theta'\cos^2\theta'\cos^2\theta_1 + \cos^4\theta'\sin^2\theta_1\cos^2\theta_1) \equiv \overline{|C|^2} \quad . \end{aligned} \tag{12}$$

Inserting this expression into Eq. (10), and replacing the summation over $\vec{k}_2$ by the integral

$$\frac{1}{N}\sum_{\vec{k}_2} \to (a/2\pi)^3 \int' k_2^2\sin\theta'\,dk_2\,d\theta'\,d\psi$$

with $\int'$ denoting the restriction $\vec{k}_3 = \vec{k}_1 + \vec{k}_2$, we have

$$\frac{1}{T_k} = \frac{\pi}{2\hbar^2 S}(4\pi g\mu_B M)^2 a^3/(2\pi)^2 \int' k_2^2\sin\theta'\,dk_2\,d\theta'\,\overline{|C|^2}(1 + \bar{n}_2)(\bar{n}_3/\bar{n}_1)\delta(\omega_1 + \omega_2 - \omega_3) \quad . \tag{13}$$

In order to remove the energy δ function, we approximate the dispersion relation for the k_3 mode by

$$\omega_3 = \gamma[H_c^2 + H_E^2 \sin^2(\tfrac{1}{2}k_3 a)]^{1/2} \ .$$

Since $\vec{k}_3 = \vec{k}_1 + \vec{k}_2$, we have

$$k_3^2 = k_1^2 + 2k_1 k_2 \cos\theta' + k_2^2 \ ,$$

which allows us to form the density of states

$$d\omega_3/d\theta' = -(k_1 k_2/k_3)(H_E^2 a/2\omega_3) \times \sin(\tfrac{1}{2}k_3 a)\cos(\tfrac{1}{2}k_3 a)\sin\theta'$$

and eliminate the integration over θ', leaving only that over k_2. The final expression is

$$\frac{1}{T_k} = \frac{4\pi}{\gamma^2 H_E^2 \hbar^2 S}(g\mu_B M)^2 \times \int_0^{\pi/a} \frac{\omega_3 a^3 k_2 k_3 \, dk_2}{k_1 a \sin(k_3 a/2)\cos(k_3 a/2)} \times |\overline{C}|^2 (1+\bar{n}_2)\bar{n}_3/\bar{n}_1 \ . \quad (14)$$

The integral of Eq. (14) was evaluated numerically by summing over 500 increments of k_2 from the zone center to the boundary, with all energies and angles restricted to satisfy energy and momentum conservation. Before discussing the results, however, it is instructive to consider qualitatively the differences between the ferromagnetic and antiferromagnetic cases.

For very small values of k_1, such that k_2 and k_3 are very nearly equal and parallel, it will not be possible to satisfy energy conservation with a finite gap in the spectrum. The minimum value $k_{1\,\min}$ for which both energy and momentum can be conserved is found approximately when the energy gap ω_0 divided by $k_{1\,\min}$ equals the maximum slope $(d\omega_k/dk)_{\max}$. This mimimum value increases with increasing gap and is also present in ferromagnets under a dc field.[9,10] The value of $(d\omega_k/dk)_{\max}$ is the same in ferromagnets and low-gap antiferromagnets with the same exchange energy, but the position is different. In ferromagnets it occurs halfway between the zone center and edge, with ω_k approximately half the exchange frequency, while in antiferromagnets, it occurs closer to the zone center and at lower frequency.

In YIG, with a much larger exchange constant than MnF_2 [$T_c(\text{YIG})/T_N(MnF_2) \sim 8$], $k_{1\,\min}$ is much smaller than in MnF_2, and seems to be experimentally undetectable. In the high-temperature, low-gap limit, where $\hbar\omega_0, \hbar\omega_{k\,\max} \ll kT$, but $kT \ll \gamma H_E$ Eq. (14) predicts a temperature dependence of $1/T_1 \propto T^{3/2}$, compared with the linear T dependence of the ferromagnet. This can be shown to arise from the linear region of the antiferromagnetic dispersion, which contains $\omega_{k\,\max}$. The linear region of $1/T_1$ vs k observed in the ferromagnet is replaced by a rather sudden increase in $1/T_1$ above $k_{1\,\min}$ to a value nearly independent of k, shown for several temperatures in Fig. 5.

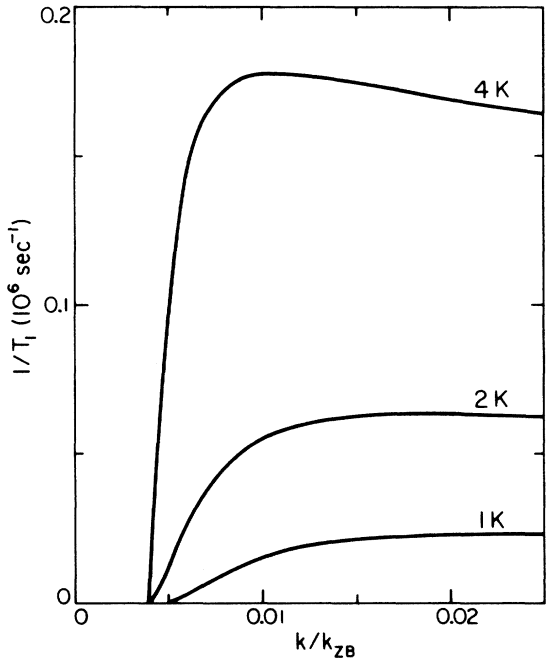

FIG. 5. Variation of the relaxation rate vs wave-vector amplitude for $\theta = \frac{1}{2}\pi$ magnons in MnF_2 at several temperatures, for the dipolar three-magnon confluence process. The results correspond to a fixed value of the applied field $H_0 = 91$ kOe so that each wave vector corresponds to a different energy.

In the low-temperature, low-gap limit, $\hbar\omega_0 \ll kT \ll \hbar\omega_{k\,\max}$, $1/T_1$ becomes dominated by the Bose factor of the incoming magnon, which becomes $\exp(-\hbar\omega_k/kT)$ near $k_{1\,\min}$. Magnons of k larger than $k_{1\,\min}$ are relaxed by thermal magnons of longer wavelength and lower energy than $\omega_{k\,\max}$, and consequently approach a value close to that given by the high-temperature limit above.

B. Four-magnon relaxation

The main mechanism for four-magnon relaxation is the exchange interaction. The four-magnon processes arising from the anisotropy interaction, however, do play an important role in that they may result in destructive interferences which decrease the rate of relaxation.[17] One must therefore treat the anisotropy carefully if a quantitative comparison between theory and experiment is to be made. In the case of MnF_2, where the anisotropy is due almost entirely to dipole-dipole interactions, one should use the magnon operators introduced in the Appendix. This would make the relaxation calculation much more complicated than if single-ion interactions were

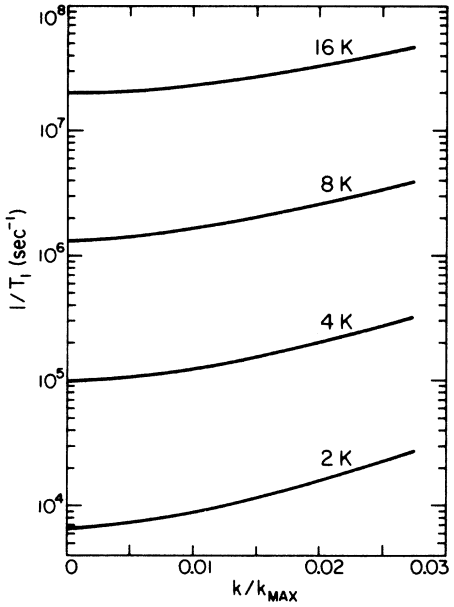

FIG. 6. Relaxation rate due to four-magnon exchange and anisotropy scattering vs wave vector in MnF_2 at several temperatures, and at fixed field $H_0 = 91$ kOe.

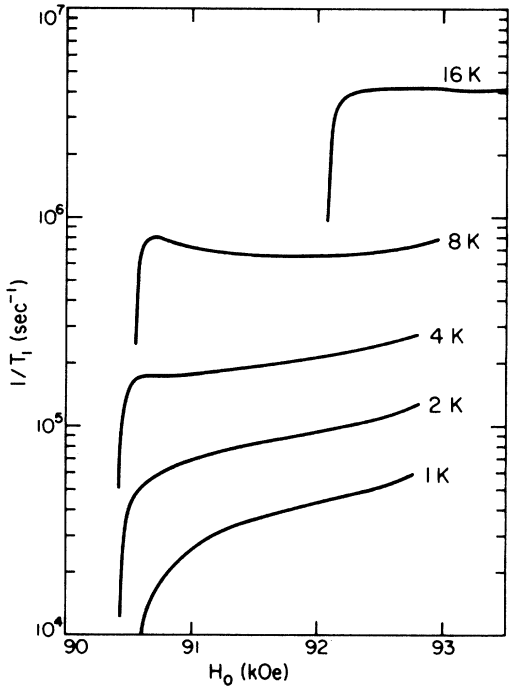

FIG. 7. Variation of the relaxation rate vs applied field for $\theta = \frac{1}{2}\pi$ magnons in MnF_2 at several temperatures, for the three-magnon confluence process. The results correspond to a fixed frequency of $f = 15.18$ GHz, so that each field corresponds to a different wave vector.

the source of the anisotropy. However, it has been shown previously[17] that an effective single-ion form of the anisotropy well describes the four-magnon relaxation rate of the $k = 0$ mode in MnF_2, and we assume this approximation to be valid for small-$\vec{k}$ magnons as well. With this simplification the four-magnon relaxation rate was calculated numerically using the procedures described in detail in Refs. 17 and 26. The results are shown as a function of k for several temperatures in Fig. 6.

It is interesting to note that these calculated results are in good qualitative agreement with the observed parallel-pumping data in $CuCl_2 \cdot 2H_2O$, as well.[15] The k dependence of the four-magnon process exhibits the form $1/T_1 = 1/T_{10} + Dk^2$, found in $CuCl_2 \cdot 2H_2O$, where both the $k = 0$ value $1/T_{10}$ and the slope D follow nearly a T^4 dependence. Although the calculation contains entirely different parameters from those appropriate to our experiment, it suggests that four-magnon processes are responsible for spin-wave relaxation in $CuCl_2 \cdot 2H_2O$.

V. DISCUSSION OF THE RESULTS

In order to compare the parallel-pumping-threshold data of Fig. 1 more directly with theory, we have calculated the relaxation rates for $\frac{1}{2}\pi$ magnons from three- and four-magnon processes at constant frequency as a function of field H_0. The value of k is now an implicit function of H_0, as is the data. The results are shown in Figs. 7 and 8. Although they

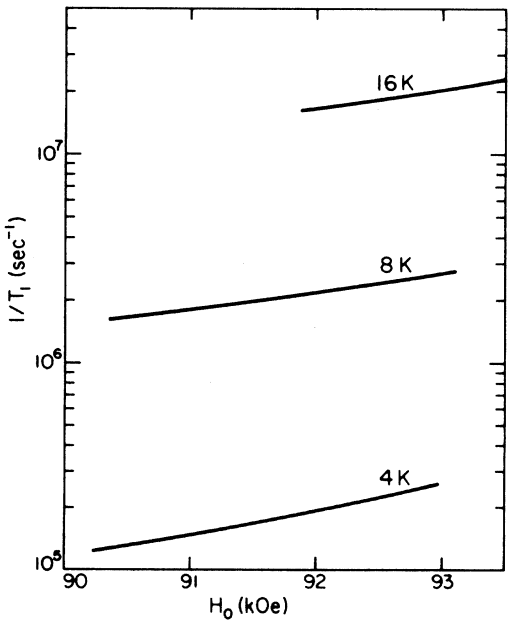

FIG. 8. Relaxation rate due to four-magnon exchange and anisotropy scattering vs field in MnF_2 at several temperatures, and at fixed frequencey $f = 15.18$ GHz.

are in reasonable numerical agreement with the data, neither the temperature nor the field dependence is fitted very well. We shall discuss these effects separately.

A. Field dependence

The three main features of the field dependence of the data can be summarized as follows: a pronounced dip at $k \sim 0$ at all temperatures; a gradual increase in the threshold with increasing field for all temperature; a shift of the curves toward higher field with increasing temperature. It is to be noted that the field dependence of the data is very similar for all temperatures, which is evidenced by the fact that the same curve was drawn through the data points at each temperature.

While the dip at low temperatures could partially be explained by the fact that the dipolar interaction cannot relax magnons with $k < k_{min}$, the same argument does not apply at higher temperatures. There, the four-magnon process is expected to dominate, and to contribute to relaxation all the way to $k = 0$. Further, if the three-magnon process vanished in the dip, we would expect to see the much stronger temperature dependence of the four-magnon process there. Thus, we are forced to conclude that the region of zero relaxation of the three-magnon is probably not the source of the dip, even at low temperatures, and we must seek other mechanism(s) for the origin of the dip. We return to this point in a later section.

At higher fields, above the dip, a gradual increase in the threshold power is observed as the field is increased toward spin flop. Although this field dependence resembles that of the three-magnon process at low temperature, neither the three- nor the four-magnon process shows much field dependence at higher temperatures. Therefore, it seems that none of the field dependence can be understood in terms of just three- and four-magnon scattering.

B. Temperature dependence

In order to separate the temperature dependence of the relaxation from its field dependence, we have replotted in Fig. 9 the data of Fig. 1, for three values of k, as a function of temperature. The three- and four-magnon rates are also shown, for corresponding frequencies and fields. Again, notice that the data show a distinct k dependence, whereas the temperature dependence at each value of k is practically identical. Hence, whatever mechanism is responsible for the relaxation in the $k \approx 0$ dip, whether it be some modified form of the three- or four-magnon processes, or another distinct process, *it must be the same as that which is responsible for the higher k relaxation.*

Below about 4 K, the observed temperature dependence of $T^{0.7}$ is considerably less rapid than the $T^{1.5}$ predicted for $k/k_{max} \simeq 0.01$. Although this can hardly be called "good agreement," the magnitude of the three-magnon process is not that far off so as to rule it out entirely as the source of the relaxation. Perhaps some modification of the process, as might be required to fit the field dependence, would also account for the discrepancy in the temperature dependence.

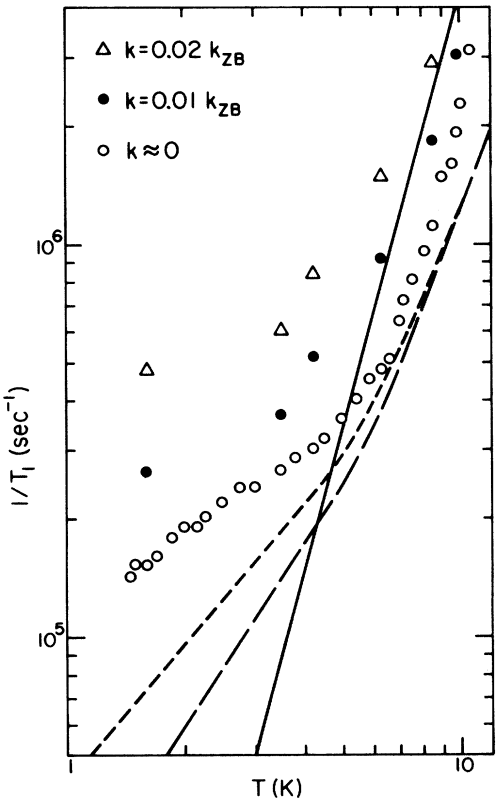

FIG. 9. Comparison of measured relaxation rates vs theory for several wave-vector amplitudes, as a function of temperatures. The rates shown are due to the three-magnon confluence process for $k = 0.01 k_{ZB}$ (long dashes) and $k = 0.02 k_{ZB}$ (short dashes), and the four-magnon exchange and anisotropy process for $k \simeq 0$.

At higher temperatures, above about 6 K, the observed temperature dependence fits very well the $T^{3.7}$ predicted by the four-magnon process, with the magnitudes in agreement within a factor of 2. Considering that the conversion from threshold power to relaxation rate depends on the knowledge of the absolute value of the rf field in the cavity, we consider the agreement to be excellent.

C. Size-dependent effects

One possible explanation for the dip is a sample-size effect. Only if the parametrically pumped mag-

nons propagate in an infinite medium, can one assume different k modes not to be coupled; in this case alone are k-mode plane waves the normal modes of the system. If the mean-free path is large enough, magnons excited in the bulk can reach the surface of the sample and be scattered into other bulk or surface modes. The effect of the surface condition or the scattering of magnons has been studied in detail.[27] In the limiting case

$$v_{Gk} T_k >> d \ , \tag{15}$$

where v_{Gk} is the magnon group velocity and d is the sample dimension, one would expect magnons with different θ_k to be strongly coupled; hence it is not meaningful to speak of a threshold for a single θ_k mode pair. In this instance, the threshold for pumping the system would be higher than that for $\theta = \frac{1}{2}\pi$ modes, as shown in Eq. (A11). In the range of temperature of our experiments, T_k is sufficiently long that condition (15) is satisfied for all $k/k_{\max} > 0.01$, in which case the threshold measured at higher fields corresponds to the excitation of modes with all θ_k values. As the field decreases, both k and the group velocity decrease as well, and the condition of Eq. (15) is no longer met. Then, only $\theta_k = \frac{1}{2}\pi$ modes are excited, and since they have lower thresholds, a pronounced dip in the curve of $h_{\rm crit}$ might appear. We have calculated the rate of Eq. (A11) for the three-magnon process, which gives a field dependence virtually identical to that in Fig. 7, for the high-field side of the butterfly curves, but with the thresholds higher by a factor of about 2. For the four-magnon process, where there is little k or θ_k dependence to the relaxation rate, the threshold would be expected to increase by a factor of about $8/\pi$. Both processes, therefore, would show a size-dependent dip of about the same magnitude. Since the relaxation rates T_k are observed to change with temperature by well over one order of magnitude, the range of values of v_{Gk}, and hence of H_0, given by the inequality [Eq. (15)], should change by a corresponding amount. One would then expect the *width* of the dip to increase rapidly with increasing temperature. This effect is clearly not observed, since the shape of the butterfly curves for all temperatures is virtually identical. Obviously, a more systematic study of the size effect is needed to verify these ideas.

VI. CONCLUSION

We have performed parallel-pumping experiments on MnF_2 at temperatures between 1.6 and 11 K, and in fields between 90 kOe and spin flop. Magnon relaxation rates have been determined, and compared with the theory of three-magnon dipolar scattering and four-magnon exchange-plus-anisotropy scattering. The low-temperature results below 4 K are in rough agreement with the temperature dependence of the three-magnon theory, while the results above 6 K are in excellent agreement with that of the four-magnon process. The field dependence of $1/T_1$ for all temperatures shows an anomalous dip near $k = 0$, which cannot be explained by ordinary (plane-wave) magnon-scattering processes. We have postulated a sample-size-dependent model which might account for the dip.

Although detailed parallel-pumping experiments have been made on $CuCl_2 \cdot 2H_2O$, the present work constitutes the first combined experimental and theoretical study of parallel pumping of purely electronic magnons in a fundamental antiferromagnet.

ACKNOWLEDGMENTS

The research at UCSB was supported by the NSF Grant No. DMR77-20185. We wish to thank Dr. R. W. Sanders for preparing the samples and Mr. Neil Nighman for growing the crystals. The work at Universidade Federal de Pernambuco is partially supported by Financiadora de Estudos e Projectos (FINEP) and Conselho Nacional de Desenvolvimento Científico e Tecnológico (CNPq).

APPENDIX: DERIVATION OF THE THRESHOLD FOR PARALLEL PUMPING OF SPIN WAVES IN ANTIFERROMAGNETS

The threshold intensity for parallel pumping of electronic spin waves in a two-sublattice antiferromagnet was first obtained by Morgenthaler[28] many years ago. His calculation, which is based on the semiclassical equations of motion for the magnetization, assumes that each magnon mode pumped by the external field decays towards equilibrium independently of the others. In this case there is a threshold for instability associated with each mode and the onset of the nonlinear excitation is determined by the minimum threshold at each value of frequency and applied field. From a more general point of view the modes can be assumed to be coupled via two-magnon processes, so that the threshold depends on the cooperative decay of the degenerate modes. Here we derive the threshold conditions based on the energy balance equations in two extreme limits, namely, in the no-coupling and in the strong-coupling regimes.

The quadratic part of the antiferromagnetic Hamiltonian including Zeeman, exchange, and magnetic-dipole interactions can be written as[23]

$$\begin{aligned}\mathcal{H}_0 = \hbar \sum_k & (A_k - \gamma H_0) a_k^\dagger a_k + (A_k + \gamma H_0) b_k^\dagger b_k \\ & + B_k (a_k b_{-k} + a_k^\dagger b_{-k}^\dagger) + C_k (a_k a_{-k} + b_k b_{-k}) \\ & + C_k (a_k^\dagger a_{-k}^\dagger + b_k^\dagger b_{-k}^\dagger) + 2C_k a_k b_k^\dagger + 2C_k a_k^\dagger b_k \ , \end{aligned} \tag{A1}$$

where

$$A_k = \gamma[H_E + H_A + \tfrac{2}{3}\pi M(1-3\cos^2\theta_k)] \ ,$$
$$B_k = \gamma[\gamma_k H_E + \tfrac{2}{3}\pi M(1-3\cos^2\theta_k)] \ ,$$
$$C_k = \gamma\pi M \sin^2\theta_k \exp(-2i\phi_k) \ .$$

In the derivation of Eq. (A1) it is assumed that the shape of the sample is spherical and that the anisotropy field H_A is due to the dipolar interaction evaluated within the Lorentz sphere. H_A is assumed to be independent of k, which is a good approximation for long-wavelength magnons. The Hamiltonian (A1) can be diagonalized by the transformation[23]

$$\begin{pmatrix} a_k \\ a^{\dagger}_{-k} \\ b_k \\ b^{\dagger}_{-k} \end{pmatrix} = \begin{pmatrix} Q_{11} & Q_{12} & Q_{13} & Q_{14} \\ Q_{21} & Q_{22} & Q_{23} & Q_{24} \\ Q_{31} & Q_{32} & Q_{33} & Q_{34} \\ Q_{41} & Q_{42} & Q_{43} & Q_{44} \end{pmatrix} = \begin{pmatrix} \alpha_k \\ \alpha^{\dagger}_{-k} \\ \beta_k \\ \beta^{\dagger}_{-k} \end{pmatrix} \ . \tag{A2}$$

The lengthy expressions for the transformation coefficients are given in Ref. 23 and the normal mode frequencies can be written as

$$\omega_{-\beta k,\alpha k} = \{A_k^2 - B_k^2 + \gamma^2 H_0^2 \pm [4(A_k^2 - B_k^2)\gamma^2 H_0^2 + 16|C_k|^2(A_k - B_k)^2]^{1/2}\}^{1/2} \ . \tag{A3}$$

When a driving rf magnetic field $h_1 \sin\omega_p t$ is applied parallel to the static field, which is assumed to lie along the axis of the crystal, the term of the Hamiltonian responsible for the excitation of α-mode magnons becomes

$$\mathcal{H}_1 = \hbar h_1 \sin\omega_p t \sum_k P_k(\alpha_k^{\dagger}\alpha_{-k}^{\dagger} + \alpha_k\alpha_{-k}) \ , \tag{A4}$$

where

$$P_k = \gamma(Q_{41}Q_{31} - Q_{21}Q_{11}) \ .$$

Since the magnon modes are driven in pairs, the occupation numbers obey the relation $n_k = n_{-k}$. Then the rate of change of n_k due to the pumping field can be written as[29]

$$\left(\frac{dn_k}{dt}\right)_p = \tfrac{1}{2}(h_1 P_k)^2(2n_k+1)\left[\frac{1/T_k}{(\omega_p - 2\omega_k)^2 + 1/T_k^2}\right] \ , \tag{A5}$$

where T_k is the (energy) relaxation time of the k mode. The time rate of change of the occupancy due to the relaxation of the magnons into the thermal modes is

$$\left(\frac{dn_k}{dt}\right)_r = -\frac{n_k - \bar{n}_k}{T_k} \ . \tag{A6}$$

In the usual calculations it is assumed that the different k modes do not interact, so that the energy balance takes place for individual modes. Using $(dn_k/dt)_p = -(dn_k/dt)_r$ and the threshold condition $n_k \to \infty$, we obtain the critical field. For the modes under resonance $\omega_p = 2\omega_k$,

$$h_c = \frac{1}{T_k}\frac{1}{|P_k|} \ . \tag{A7}$$

Using the expressions for the transformation coefficients, Eq. (A7) becomes

$$h_c = \frac{(\omega_{\alpha k} - \gamma H_0)[A_k^2 - B_k^2 - (\omega_{\alpha k} + H_0)^2]^2 + 16|C_k|^2(A_k - B_k)^2(\omega_{\alpha_k} + \gamma H_0)}{\gamma T_k 4\gamma H_0 C_k(A_k - B_k)[A_k^2 - B_k^2 - (\omega_{\alpha k} + \gamma H_0)^2]} \ . \tag{A8}$$

Note that if the dipolar interaction is neglected, the transformation coefficients in Eq. (A2) become $Q_{11} = u_k$, $Q_{21} = Q_{31} = 0$, $Q_{41} = v_k$. In this case $P_k = 0$ and the threshold field diverges. This is so because it is the dipolar interaction that makes the spin precession of the $\theta_k \neq 0$ modes to be elliptical, which is the necessary condition for the coupling between the z-directed pumping field and the rf magnetization. If we assume that H_A, $\omega_\alpha/\gamma \ll H_E$, H_c, Eq. (A8) simplifies greatly to give

$$h_c = \frac{1}{\gamma T_k}\frac{\omega_{\alpha k}(2H_E)^{1/2}}{\gamma\pi M \sin^2\theta_k[H_A + H_E(1-\gamma_k)]^{1/2}} \ . \tag{A9}$$

This is the same result obtained by Morgenthaler.[28] Note that for long-wavelength magnons $\gamma_k \simeq 1$, so that the threshold is inversely proportional to $H_A^{1/2}$. It is for this reason that parallel pumping of electronic magnons has not been observed in the well-studied low-anistropy antiferromagnets, such as $RbMnF_3$ and $KMnF_3$.

In a situation where the degenerate magnon modes with $\omega_k = \frac{1}{2}\omega_p$ pumped by the rf field are strongly coupled one cannot assume that the different k modes provide independent channels for the energy flow. The coupling between the modes may arise from two-magnon interaction due to surface pit scattering. In this case the condition for the coupling to be effective is that the mean free path $\lambda_k = v_{Gk}T_k$ be comparable or larger than the dimension of the sample. The energy balance equation must now account for the total energy flowing in and out of the pumped modes, i.e.,

$$\sum_k \left(\frac{dn_k}{dt}\right)_p = -\sum_k \left(\frac{dn_k}{dt}\right)_r \ , \tag{A10}$$

where the sum is restricted to the modes which satisfy $\omega_k = \frac{1}{2}\omega_p$. Of course in order to find the threshold for the collective instability, one must now consider the details of the coupling. The problem then becomes quite complicated and only in limiting situations, one hopes to find a solution. One case which can be easily solved is that of a strong coupling between the degenerate modes. If we denote by T_2 the time for a magnon to decay into the degenerate modes by two-magnon scattering, this case corresponds to $T_2 \ll T_k$. We further assume that the Fourier transform of the two-magnon scattering potential is flat in the region of interest in k space. In this case, the thermalization of the degenerate modes occurs rapidly and assures that they all have the same population $n_k = n_{k'} = n_{\omega_p/2}$. The occupation number can thus be factorized in Eq. (A10). Assuming $\omega_p = 2\omega_k$, H_A, $\omega_{\alpha k}/\gamma \ll H_E$, H_c, $\gamma_k = 1$, the condition for the collective instability of all the degenerate modes $n_{\omega_p/2} \rightarrow \infty$ yields

$$h_c = \frac{\omega_k}{\gamma^2 \pi M}\left(\frac{2H_E}{H_A}\right)^{1/2}\left(\frac{\sum_k 1/T_k}{\sum_k \sin^4\theta_k T_k}\right)^{1/2} . \qquad \text{(A11)}$$

[1]C. G. Windsor, D. H. Saunderson, and E. Schedler, Phys. Rev. Lett. 37, 855 (1976).
[2]D. D. Sell, R. L. Greene, and R. M. White, Phys. Rev. 158, 489 (1967).
[3]P. A. Fleury and R. Loudon, Phys. Rev. 166, 514 (1968).
[4]F. Barocchi, P. Mazzinghi, V. Tognetti, and M. Zoppi, Solid State Commun. 25, 241 (1978).
[5]H. Suhl, J. Phys. Chem. Solids 1, 209 (1957).
[6]A. Platzker and F. R. Morgenthaler, Phys. Rev. Lett. 26, 442 (1971).
[7]F. R. Morgenthaler, J. Appl. Phys. 31, 955 (1960).
[8]E. Schlomann, J. J. Green, and U. Milano, J. Appl. Phys. 31, 3865 (1960).
[9]M. Sparks, *Ferromganetic Relaxation Theory* (McGraw-Hill, New York, 1964).
[10]M. Sparks, Phys. Rev. 160, 364 (1967).
[11]L. W. Hinderks and P. M. Richards, Phys. Rev. 183, 575 (1969).
[12]L. W. Hinderks and P. M. Richards, J. Appl. Phys. 42, 1516 (1971).
[13]R. B. Woolsey and R. M. White, Phys. Rev. 188, 313 (1969).
[14]E. A. Soares and S. M. Rezende, Phys. Rev. B 15, 4497 (1977).
[15]Hitoshi Yamazaki, J. Phys. Soc. Jpn. 32, 1227 (1972).
[16]J. P. Kotthaus and V. Jaccarino, Phys. Rev. Lett. 28, 1649 (1972); *Proceedings of the 18th Conference on Magnetism and Magnetic Materials, Denver, 1972,* edited by C. D. Graham, Jr., and J. J. Rhyne, AIP Conf. Proc. No. 10 (AIP, New York, 1973), p. 57 ; J. P. Kotthaus, R. Sanders, and V. Jaccarino, *Proceedings of the International Conference on Magnetism, Moscow, 1973* (Navka, Moscow, 1974), Vol III, p. 255. Preliminary results on parallel pumping in MnF_2 are reported in the latter paper.
[17]S. M. Rezende and R. M. White, Phys. Rev. B 14, 2939 (1976).
[18]V. E. Zakharov, V. S. L'vov, and S. S. Starobinets, Sov. Phys.-Usp. 17, 896 (1975).
[19]R. Loudon and P. Pincus, Phys. Rev. 132, 673 (1963); the Lorentz correction is given in A. B. Harris, Phys. Rev. 143, 353 (1966).
[20]S. M. Rezende, A. R. King, R. M. White, and J. P. Timbie, Phys. Rev. B 16, 1126 (1977).
[21]J. Barak, V. Jaccarino, and S. M. Rezende, J. Magn. Magn. Mater. 9, 323 (1978).
[22]A. R. King and D. Paquette, Phys. Rev. Lett. 30, 662 (1973).
[23]A. B. Harris, D. Kumar, B. I. Halperin, and P. C. Hohenberg, Phys. Rev. B 3, 961 (1971).
[24]R. B. Woolsey and R. M. White, Int. J. Magn. 2, 51 (1972).
[25]D. Beeman and P. Pincus, Phys. Rev. 166, 359 (1968).
[26]S. M. Rezende and R. M. White, Phys. Rev. B 18, 2346 (1978).
[27]See E. Sawado, Phys. Rev. B 14, 174 (1976), and references therein.
[28]F. R. Morgenthaler, J. Appl. Phys. 36, 3102 (1965).
[29]R. M. White and M. Sparks, Phys. Rev. 130, 632 (1963).